Ecological impact of the antibiotic ciprofloxacin on microbial community of aerobic activated sludge

Dogun Kim · Luong N. Nguyen · Seungdae Oh

Abstract This study investigated the effects and fate of the antibiotic ciprofloxacin (CIP) at environmentally relevant levels (50–500 µg/L) in activated sludge (AS) microbial communities under aerobic conditions. Exposure to 500 µg/L of CIP decreased species diversity by about 20% and significantly altered the phylogenetic structure of AS communities compared to those of control communities (no CIP exposure), while there were no significant changes upon exposure to 50 µg/L of CIP. Analysis of community composition revealed that exposure to 500 µg/L of CIP significantly reduced the relative abundance of *Rhodobacteraceae* and *Nakamurellaceae* by more than tenfold. These species frequently occur in AS communities across many full-scale wastewater treatment plants and are involved in key ecosystem functions (i.e., organic matter and nitrogen removal). Our analyses showed that 50–500 µg/L CIP was poorly removed in AS (about 20% removal), implying that the majority of CIP from AS processes may be released with either their effluents or waste sludge. We therefore strongly recommend further research on CIP residuals and/or post-treatment processes (e.g., anaerobic digestion) for waste streams that may cause ecological risks in receiving water bodies.

Introduction

Antibiotics are widely used for preventing or treating microbial infections in humans and for veterinary applications. Although antibiotics are indispensable in modern society, their increasing use has led to their presence in a variety of water environments. Since antibiotics are designed to be biologically active, antibiotic residues in water environments not only severely affect aquatic ecology, but also promote microorganisms that are persistent/resistant to antibiotics. Among others, ciprofloxacin (CIP) is of growing concern and represents a health hazard for aquatic life. CIP was introduced in the 1980 s and has become one of the most commonly used antibiotic quinolones for human and animal antibacterial therapies. The majority of CIP, after its usage, is thought to be released into urban waste streams through sewage disposal, and most of it is eventually collected in wastewater treatment plants (WWTPs), as consistent with the

D. Kim · S. Oh (✉)
Department of Civil Engineering, Kyung Hee University,
1732 Deogyeong-daero, Giheung-Gu, Yongin-Si,
Gyeonggi-do 17104, Republic of Korea
e-mail: soh@khu.ac.kr

L. N. Nguyen
Center for Technology in Water and Wastewater, School
of Civil and Environmental Engineering, University of
Technology Sydney, Sydney, NSW 2007, Australia

highest loads detected in wastewater-associated environments (Larsson et al. 2007; Fick et al. 2009).

While CIP is readily detectable in many aquatic environments (typically found at ng/L-μg/L levels in surface waters) (Sahlin et al. 2018), it occurs at high levels in the effluents of WWTPs (up to 6.5–31 mg/L) receiving pharmaceutical wastewaters and in rivers (up to 14 mg/L) contaminated with industrial waste (Larsson et al. 2007; Fick et al. 2009). Freshwater primary producers such as cyanobacteria (*Microcystis aeruginosa*) and duckweed (*Lemna minor*) are inhibited by CIP at 17–203 μg/L (Robinson et al. 2005); 5–50 mg/kg of CIP reduces the diversity of soil microbial communities (Girardi et al. 2011; Cui et al. 2014); and 100 μg/L of CIP reduces the nitrifying activities of freshwater microbial communities (Rico et al. 2014). Johansson et al. (2014) found that 18–199 μg/L of CIP inhibited the metabolic activities (e.g., substrate utilization) of a periphyton community comprising a variety of autotrophic and heterotrophic organisms.

CIP at varied levels also disrupts the structure and function of microbial communities in engineered biological systems, such as WWTPs. High level of CIP (0.5 mg/L) causes significant alteration in the phylogenetic structure of methanogenic microbial communities, significantly decreasing methane production by inhibiting *Syntrophobacter* and *Methanothrix* associated with acetogenesis and acetoclastic methanogenesis, respectively (Mai et al. 2018). Yi et al. (2017) found that biological removal of nitrogen (particularly with denitrification) and phosphorous was reduced with 2 mg/L of CIP in laboratory microcosm settings. Although several studies suggest that CIP at environmentally relevant levels causes perturbations in ecosystem functions in engineered systems, whether and how CIP causes toxicity in the structure and functions (e.g., heterotrophic activities) of activated sludge (AS) communities under aerobic conditions remain to be clearly elucidated.

Since CIP concentrations detectable in the environment can exceed the toxicity thresholds of many aquatic organisms, satisfactory treatment of CIP in WWTPs is highly desired. Removal rates of CIP in WWTPs are greatly variable, ranging from 20% to 95% in conventional activated sludge (CAS) processes (Verlicchi et al. 2012). Among other factors, the input level of a contaminant could affect its fate and removal in CAS processes (Nguyen and Oh 2019). Although

there is a wealth of data on the behavior of CIP in CAS processes under relatively low input levels (e.g., < 10 μg/L) (Sahlin et al. 2018), little is known about the fate of CIP at high levels that may represent spatiotemporal peaks and/or accidental spills from industrial waste streams. Hence, this study is a systematic investigation of the fate of CIP in AS at 50–500 μg/L, which is higher than the typical level (mean/median) in wastewaters but less than environmental maxima (e.g., industrial inputs). We established a total of nine AS-inoculated laboratory bioreactors receiving influents with various levels of CIP and performed quantitative assessments on the removal rates of CIP. We also conducted 16S rRNA gene sequencing and analysis of AS communities to describe microbial community dynamics under CIP exposure, and we documented the potential disruption of AS ecosystem functions.

Materials and methods

Materials

Analytical-grade (> 98% purity) ciprofloxacin hydrochloride monohydrate was purchased from Sigma-Aldrich (Singapore). A stock solution of 1 g/L CIP was prepared in Milli-Q water and stored at 4 °C prior to use. A synthetic feed containing $C_6H_{12}O_6$ (1.83 g), NH_4Cl (30 mg), KH_2PO_4 (340 mg), K_2HPO_4 (600 mg), $MgSO_4 \cdot 7H_2O$ (270 mg), $FeSO_4$ (10 mg), and 10 mL of 100 × trace element solution ($ZnSO_4 \cdot 7H_2O$ 0.35 mg, $MnSO_4 \cdot H_2O$ 0.21 mg, H_3BO_4 2.1 mg, $CoCl_2 \cdot 2H_2O$ 1.4 mg, $CuCl_2 \cdot 2H_2O$ 0.07 mg, $NiSO_4 \cdot 6H_2O$ 0.1 mg, $Na_2MoO_4 \cdot 2H_2O$ 0.21 mg per liter) per one liter was prepared. The ratio of chemical oxygen demand (COD), total nitrogen, and total phosphorous (COD: TN: TP) of the synthetic feed was 80: 5: 1 (Nguyen and Oh 2019).

Bioreactor development

Aerobic AS was collected from an aeration basin of a local municipal WWTP in Singapore. The WWTP included aerobic and anoxic tanks where biological nitrogen removal occurred via conventional nitrification–denitrification processes. First, we developed three control bioreactors by inoculating the AS and maintained them with synthetic feed (no CIP

exposure). The three control bioreactors were acclimated to laboratory conditions for a month, after which they showed stable COD removal and mixed liquor volatile suspended solids (MLVSS) concentration. After the acclimation period, we developed two additional sets of three bioreactors by inoculating the biomass from the control bioreactors, which were fed the synthetic feed plus either 50 µg/L of CIP (CIP_{50}) or 500 µg/L of CIP (CIP_{500}). The three sets of triplicate bioreactors ($n = 9$), consisting of the control ($n = 3$), CIP_{50} ($n = 3$), and CIP_{500} ($n = 3$), maintained the same operational conditions (except the CIP level fed) for an additional two months. The bioreactors (0.9 L working volume) were operated in sequential batch mode, consisting of 10 min of filling, about 3.5 days of reacting, and 20 min of decanting without settling. One-third of the mixed liquor suspension was withdrawn (decanting process) and replaced with a freshly prepared synthetic feed (filling process) twice a week. The bioreactors were operated at 22 ± 1 °C and 3–4 mg/L of dissolved oxygen (aerated using air diffusers). The solid retention time and organic loading rate were 10.5 days and 0.4 kg COD/m³/day, respectively, comparable to those of many full-scale AS processes.

Analytical methods

Organic matter removal and heterotrophic growth of AS microbial communities were assessed using soluble COD (sCOD) and MLVSS measurements, respectively. The sCOD was measured using a HACH colorimetric method after filtering the samples through a 0.22-µm filter. MLVSS were measured following the standard method (APHA 1998). To determine CIP concentration, a high-performance liquid chromatography system (Shimadzu Asia Pacific Pte. Ltd., Singapore) equipped with a Shim-Pack GIST Phenyl column (5 µm, 4.6 × 250 mm) and a UV–vis multiple wavelength detector was used. The mobile phase was composed of 60% acetonitrile and 40% Milli-Q water buffered with 25 mM NaH_2PO_4 at a pH of 2.5. The mobile phase was delivered at 1.8 mL/min through the column for 5 min. CIP was eluted and detected at 3.5 min and 280 nm, respectively. The limit of quantification for CIP using these conditions was approximately 10 µg/L. The CIP removal rates (R, %) in the bioreactors were calculated using Eq. (1):

$$R = \frac{C_i - C_e}{C_i} \times 100 \tag{1}$$

where C_i and C_e denote the concentration of CIP in the influent and effluent, respectively.

CIP concentration adsorbed on the AS was analyzed using ultrasonic solvent extraction (Wijekoon et al. 2013; Nguyen and Oh 2019). Briefly, AS samples were freeze-dried for more than 5 days and ground to fine particles with a spatula. A certain amount of particles was mixed with 5 mL of methanol with a vortex mixer and then was ultrasonicated for 10 min. The resultant suspension was centrifuged at $2851 \times g$ for 10 min, and the supernatant was collected. The remaining solid mixture was subjected to another round of extraction. The supernatants from all rounds of extractions were mixed together and filtered using a 0.22-µm polytetrafluoroethylene (PTFE) filter, and the CIP concentration was measured using a HPLC system. Independent tests using heat-inactivated biomass and abiotic settings showed an extraction efficiency (E) of $74 \pm 5\%$. The mass of CIP adsorbed on the AS (C_A, µg) was calculated using Eq. (2):

$$C_A = \frac{V_E - C_E}{W \times (E/100)} \tag{2}$$

where V_E (mL), C_E (µg/mL), W (g), and E (%) denote the total volume of the supernatant, the concentration of CIP in the supernatant, the mass of sludge subjected to extraction, and the extraction efficiency, respectively.

Microbial community analysis

Triplicate sludge samples were collected from control reactors at day 0 and from the three sets of bioreactors (control, CIP_{50}, and CIP_{500}) at steady state (day 42). A total of 12 samples were subjected to a DNA extraction protocol using a PowerSoil® DNA isolation kit (MOBIO, Carlsbad, CA, USA). The concentration of extracted DNA was analyzed with a NanoDrop 2300 spectrophotometer (ThermoFisher Scientific) and agarose gel electrophoresis. The concentration and absorbance ratio (A_{260}/A_{280}) of all DNA samples was higher than 0.5 µg/µL and 1.8, respectively. The hypervariable region (V3-V4) of the 16S rRNA genes was amplified using universal bacterial primers (341F-805R; Macrogen Inc., Seoul, Republic of Korea). The MiSeq™ platform at Macrogen Inc. was used for

sequencing. Paired-end (2 × 300 bp) 16S rRNA gene sequences were created and analyzed using the MiSeq^{TM} SOP pipeline (Kozich et al. 2013), as described previously (Oh and Choi 2018). The parameters used were no ambiguous sequence, > 200 bp in length, and < 8 bp homopolymer; the others were at default settings. The preprocessed sequences were chimera-checked using chimera.vsearch and then taxonomically classified with classify.seqs. Chimeric sequences and those assigned to chloroplasts, mitochondria, archaea, eukaryotes, and unknown were excluded from further analyses. The remaining sequences were clustered into operational taxonomic units (OTUs) using dist.seqs and clusters with a nucleotide identity cutoff of 97%. For estimating alpha diversity indices, the number of sequences across datasets was rarefied to the lowest number per sample. Beta diversity across datasets was estimated using bacterial community composition data at the OTU level. Differential community characteristics were assessed using the Mann–Whitney U test.

Nucleotide sequence accession number

The 16S rRNA gene sequence datasets created in this study were deposited in GenBank under the following accession numbers: CIP$_{50\_1}$ (SRS2340180), CIP$_{50\_2}$ (SRS2340182), CIP$_{50\_3}$ (SRS2340184), CIP$_{500\_1}$ (SRS2340177), CIP$_{500\_2}$ (SRS2340179), CIP$_{500\_3}$ (SRS2340181), Control$_1$ (SRS2340183), Control$_2$ (SRS2340176), Control$_3$ (SRS2340220), Control$_4$ (SRS2340175), Control$_5$ (SRS2340198), and Control$_6$ (SRS2340197).

Results and discussion

Effects of CIP on the structure and diversity of AS microbial communities

The three sets of bioreactors were adapted to different CIP levels: control (no CIP exposure), 50 μg/L of CIP (CIP$_{50}$), and 500 μg/L of CIP (CIP$_{500}$) over 70 days. Mixed liquor samples from the bioreactors were collected at day 42 (steady state) and subjected to 16S rRNA gene sequencing and analysis. The bacterial community composition at the OTU level was used to perform non-metric multidimensional scaling (NMDS) analysis (Fig. 1a). The communities in each

group were clustered closely. The average similarity of the phylogenetic structures using the Bray–Curtis distance metric was 0.40 ± 0.28 (within control), 0.69 ± 0.05 (CIP$_{50}$), and 0.65 ± 0.04 (CIP$_{500}$). Communities showed a substantial distance in community structure among the three groups; the average similarities were 0.32 ± 0.14 (control vs. CIP$_{50}$), 0.24 ± 0.09 (control vs. CIP$_{500}$), and 0.41 ± 0.04 (CIP$_{50}$ vs. CIP$_{500}$). A permutational multivariate analysis of variance (PERMANOVA) test showed that the phylogenetic structure of the CIP$_{500}$ communities differed significantly from those of the control (Bonferroni-corrected $P < 0.05$). These results suggested that CIP at 500 μg/L could alter the structure of AS, while there was no significant change with 50 μg/L of CIP.

The shifts in phylogenetic structure (beta diversity) of the CIP$_{500}$ communities (Fig. 1a) further called for examining the effects of CIP on alpha diversity indices among the communities. The average Chao1 (species richness index) of the control was 272 ± 30, which was comparable to those of the CIP$_{50}$ and CIP$_{500}$ communities (Fig. 1b). The Shannon diversity index found in the control communities was 3.2 ± 0.3. The index value largely decreased ($P < 0.05$) to that of CIP$_{500}$ (2.6 ± 0.3) (Fig. 1c), suggesting a significant reduction in species diversity, while there was no substantial change (3.2 ± 0.1) found between control and CIP$_{50}$ communities. Overall, 16S rRNA gene sequencing analysis of both the alpha and beta diversity showed that exposure to 500 μg/L of CIP could severely affect the structure and diversity of AS communities.

Bacterial community diversity could be described by alpha diversity indices, including the number (richness), equitability (evenness), and diversity of community members (taxa). The results of this work clearly indicated significant reduction (about 20%) in the species diversity index under two months of exposure to 500 μg/L of CIP. Although some studies have reported that high diversity is not necessarily beneficial, a large body of literature suggests that high diversity is associated with functional diversity and ecosystem stability (Zhou and Ning 2017). Communities containing diverse members likely have more functional capacity with a versatile repertoire of metabolic pathways, which enables more stable and robust community ecosystem functions. For example, the structure and diversity of microbial communities
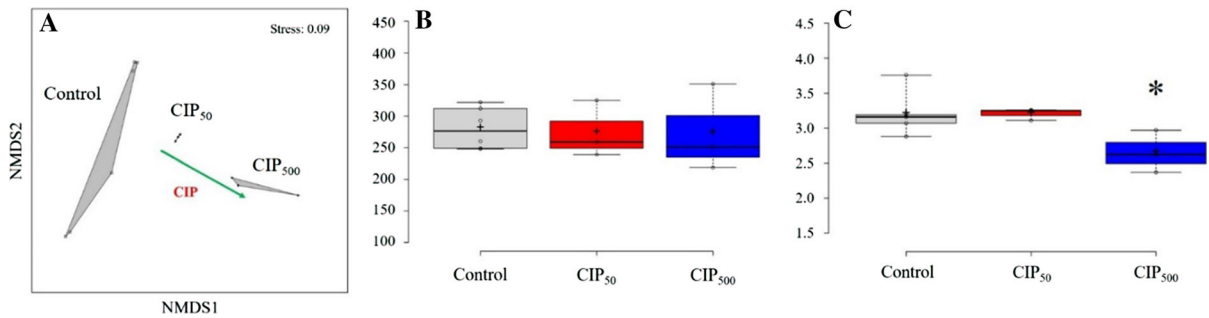
Fig. 1 Shifts in phylogenetic structure and diversity of AS communities during exposure to CIP. **a** Non-metric multidimensional scaling (NMDS) ordination plot using the Euclidean distance metric. Open circles, open squares, and solid squares represent the control ($n = 6$), CIP_{50} ($n = 3$), and CIP_{500} ($n = 3$) communities, respectively. The green arrow indicates variability of CIP. **b** Chao1 indices (species richness). **c** Shannon indices (species diversity). The box plots depict the medians (the central horizontal lines), inter-quartile ranges (boxes), data points (small open circles), means (crosses), and 95% confidence intervals (whiskers). The asterisks indicate statistical significance ($P < 0.05$ by the Mann–Whitney U test) compared to the control communities

in anaerobic digesters in full-scale WWTPs are strongly related to system performance; highly diverse communities show high methane production and substrate removal efficiency (Werner et al. 2011). Since the alpha and beta diversity indices could represent outcomes of ecological processes (e.g., selection) enacted under environmental stressors (CIP exposure), we further explored the underlying mechanisms resulting in the significant shifts in structure and diversity of AS communities under CIP exposure.

Alteration of community composition in AS: implications for AS ecosystem functions

Figure 2 shows the relative abundance of the bacterial communities at the phylum level. Overall, *Proteobacteria* (68.6, 45.6, and 64.1% for the control, CIP_{50}, and CIP_{500} communities, respectively) dominated the communities, followed by *Bacteroidetes* (16.5, 36.8, and 25.8%), *Verrucomicrobia* (3.6, 8.1, and 2.8%), and *Actinobacteria* (3.8, 3.0, and 3.1%). These phyla are known to occur frequently across many full-scale WWTPs (Zhang et al. 2018). In response to the CIP, *Bacteroidetes* slightly increased, whereas the other major phyla decreased; the shifts in relative abundance were not statistically significant ($P > 0.05$).

Further analysis of bacterial taxa identified 16 major families among the three groups of communities (Fig. 3). *Caulobacteraceae* was the most dominant in the control (16.6%), followed by *Enterobacteriaceae* (10.9%), *Ohtaekwangia* (8.8%), *Pseudomonadaceae*

(8.3%), *Flavobacteriaceae* (5.9%), *Chitinophagaceae* (5.6%), *Aeromonadaceae* (3.6%), *Comamonadaceae* (2.4%), *Verrucomicrobiaceae* (2.4%), and *Rhodobacteraceae* (2.2%). These families are often found in full-scale WWTPs with various biological unit processes (e.g., oxidation ditch, sequencing batch reactors, and membrane bioreactors) as well as CAS processes (Isazadeh et al. 2016; Saunders et al. 2016; Shchegolkova et al. 2016). Among those enriched with CIP, *Alcaligenaceae* increased significantly ($P < 0.05$) in both the CIP_{50} and CIP_{500} communities, strongly suggesting that exposure to CIP provides competitive fitness to the taxon.

Alcaligenaceae are a member of *Burkholderiales*, which are widely found in water, soil, humans, and animals. *Alcaligenaceae* carry an array of genes associated with metabolism of antibiotics and many toxic compounds, and they are often found in contaminated sites where they play a role as xenobiotic degraders (Ghosh et al. 2011). Hence, our 16S rRNA gene sequence-based community profiling results encourage future investigations on isolation of *Alcaligenaceae* followed by phenotypic characterization associated with CIP (e.g., degradation of and resistance to CIP), which will help better elucidate its exact role in communities exposed to CIP.

Nakamurellaceae and *Rhodobacteraceae* were significantly underrepresented ($P < 0.05$) in the CIP_{500} communities. Only one genus, *Nakamurella*, belonging to the family *Nakamurellaceae*, was identified in the three communities (Fig. 4), and it was significantly reduced (15-fold) in the CIP_{500} communities
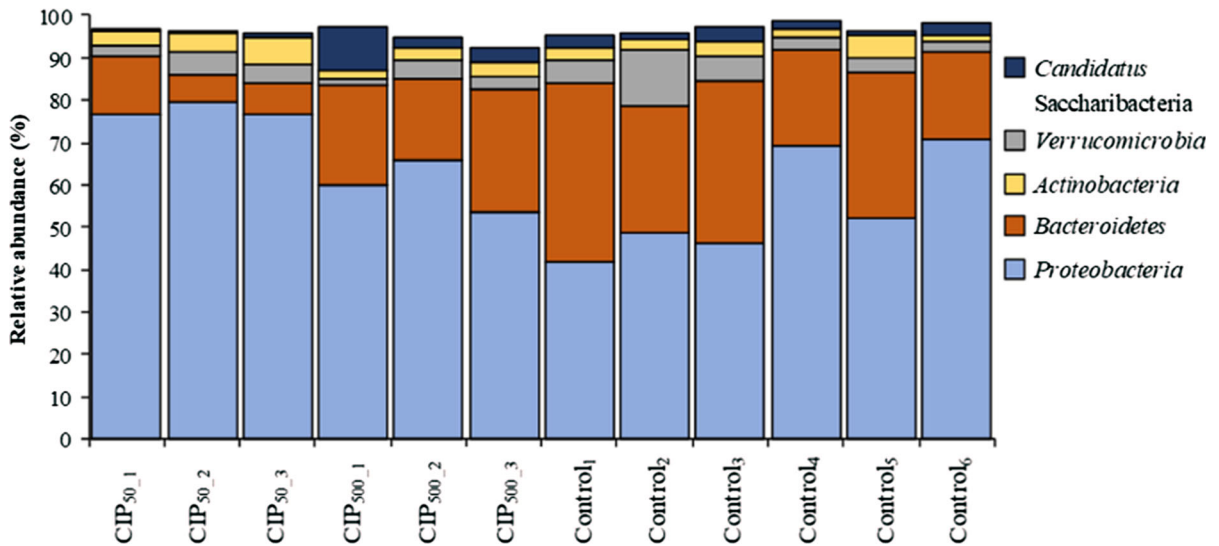
Fig. 2 Relative abundance of major phyla (> 2% on average). $Control_{1-3}$ and $Control_{4-6}$ were sampled from the triplicate control reactors at day 0 and 42, respectively. CIP_{50} and CIP_{500} were from the triplicate reactors fed 50 and 500 μg/L of CIP, respectively
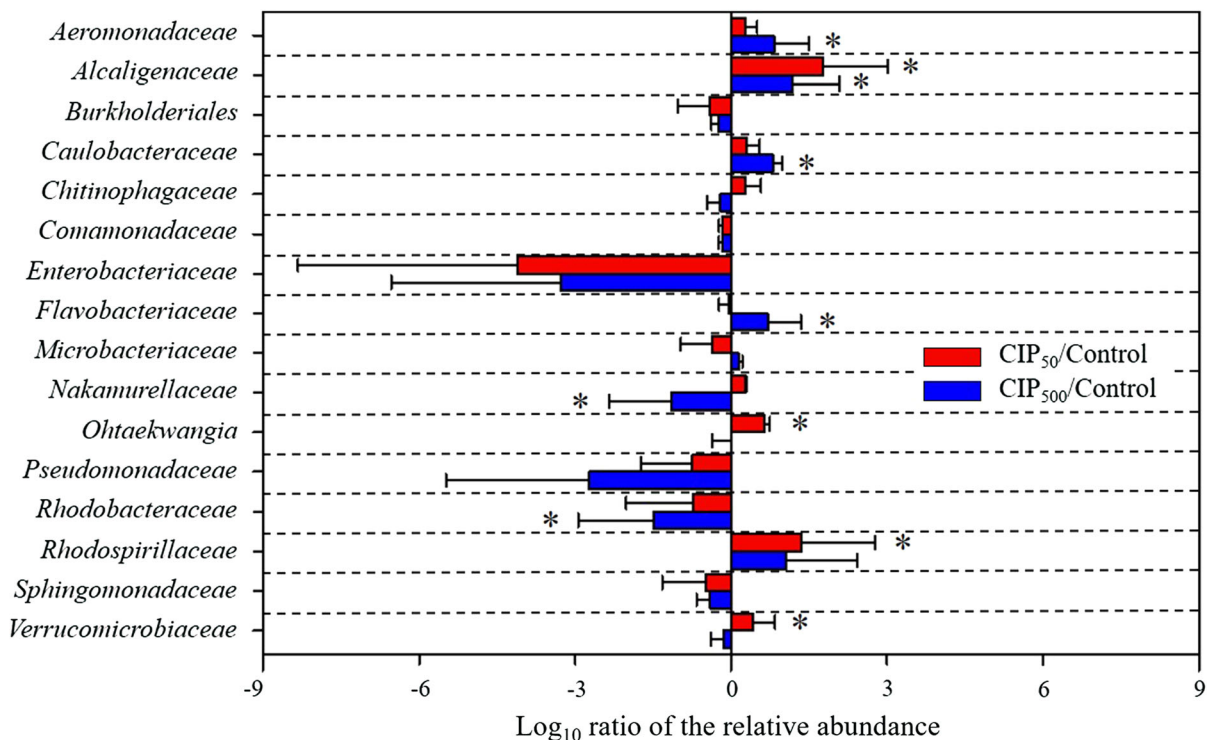
Fig. 3 Log_{10}-transformed ratio of relative abundance between the communities. Sixteen major families (> 0.5% of the average relative abundance) are shown. The log_{10}-transformed relative abundance value represents the logarithm of the relative abundance ratio (CIP-exposed communities [$n = 3$] divided by control [$n = 6$]) in base 10. The bar and error bar represent the mean and standard deviation, respectively. The asterisk indicates differential abundance with statistical significance ($P < 0.05$) between the CIP-exposed and the control communities
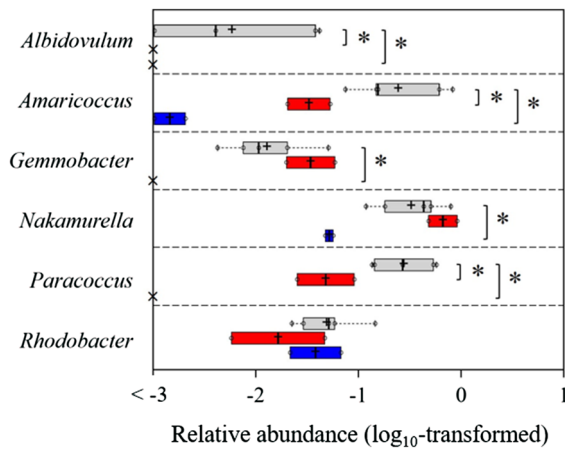
Fig. 4 Relative abundance of major genera belonging to *Nakamurellaceae* and *Rhodobacteraceae*. Gray, red, and blue boxes indicate the relative abundance of the control ($n = 6$), CIP_{50} ($n = 3$), and CIP_{500} ($n = 3$) communities, respectively. The asterisk represents differential abundance ($P < 0.05$) between the CIP-exposed and control communities. The box plots depict the medians (the central horizontal lines), inter-quartile ranges (boxes), data points (small open circles), means (crosses), and 95% confidence intervals (whiskers). X symbols indicate $< 10^{-3}$ %

compared to control. Pharmaceutical compounds such as CIP induce oxidative stresses (generating reactive oxidative species such as O_2^- and H_2O_2) in cells (Goswami et al. 2006), which cause various cellular damages (e.g., loss of membrane integrity). Given that pharmaceuticals-mediated oxidative stresses could dramatically reduce *Nakamurella* in AS communities (Jiang et al. 2017), *Nakamurella* were likely particularly sensitive to CIP-mediated oxidative stresses in addition to the known mode of action of CIP (inhibition of DNA topoisomerase II/IV activities).

Nakamurella are Gram-positive, non-motile, and non-spore-forming bacteria with an aerobic chemoorganotrophic metabolism (Nouioui et al. 2017). *Nakamurella* have been isolated from AS and are capable of accumulating a large amount of polysaccharides in cells (Yoshimi et al. 1996). Members of AS communities capable of rapid uptake and accumulation of organic matters would predominate in WWTPs. Polysaccharide-accumulating bacteria would be particularly selective in WWTPs by rapidly uptaking reserve materials of wastewaters, such as glycogen and polyphosphate, and later metabolizing them for cell body synthesis. Since the majority of soluble organic matters in wastewaters is removed by

cellular uptake in aerobic tanks, followed by separation of cells from wastewater effluents in settlers, the presence of those polysaccharide-accumulating bacteria in AS would be directly associated with the important process performance of WWTPs. Meanwhile, *Nakamurella* is a putative glycogen-accumulating organism (GAO) (Stokholm-Bjerregaard et al. 2017), which may compete with phosphate-accumulating organisms (PAOs) for carbon sources in enhanced biological phosphorus removal (EBPR) processes. Accordingly, further experiments on the physiology of *Nakamurella* and its interaction with PAOs will help better assess its exact role and contribution to the system performance of EBPR processes.

Rhodobacteraceae decreased significantly from the control ($4.0 \pm 2.8\%$) to the CIP_{500} communities ($0.1 \pm 0.1\%$). While *Rhodobacteraceae* are associated with many ecosystem functions (e.g., removal of organic matter, phosphorous, and nitrogen compounds) in AS (Saunders et al. 2016), four genera (*Albidovulum*, *Amaricoccus, Gemmobacter,* and *Paracoccus*) of *Rhodobacteraceae* were significantly ($P < 0.05$) reduced in the CIP_{500} communities (Fig. 4). *Paracoccus* decreased 11-fold with CIP_{50} and more than 70-fold with CIP_{500} compared to control. Both *Paracoccus* and *Nakamurella* are facultative anaerobic denitrifiers, and both were adversely affected by CIP. *Paracoccus* are heterotrophic anaerobes carrying genes expressing catalytic reductases for various nitrogen compounds (nitrate, nitrite, nitric oxide, and nitrous oxide), enabling complete reduction of nitrate to N_2 under micro-oxic and anoxic conditions (Bergaust et al. 2010). *Paracoccus* are primarily responsible for denitrification in aqueous and soil environments (DeVries and Zhang 2016). In addition, *Nakamurella* are capable of denitrifying and often occur in AS and other biological processes (e.g., sequencing batch reactors) (Jiang et al. 2017). The relative abundances of *Nakamurella* and *Paracoccus* are positively correlated with the denitrification rates in municipal WWTPs (Jiang et al. 2017; Zielińska et al. 2016), implying the contribution of both taxa to biological nitrogen removal.

A previous study by Yi et al. (2017) showed experimental validation of CIP-mediated perturbation at 0.2–2 mg/L CIP for both denitrification efficiency and activity of nitrite reductase, consistent with our 16S rRNA gene-based results. Accordingly, the

selective decrease of taxa identified in this study and their demonstrated phenotypes collectively suggested that CIP disrupts nitrogen removal processes in the biological unit processes of WWTPs. Biological nitrogen removal processes employed in many full-scale WWTPs involve nitrification as well as denitrification, and AS microbial communities under aerobic conditions carry out both organic matter removal and biological conversion of ammonia to nitrate, the latter of which is essential for successful nitrogen removal in WWTPs. We therefore encourage future investigations that examine whether (and at what level) CIP causes ecological perturbations on the diversity and functions of nitrifying AS communities, which will enable more accurate risk assessments on the ecotoxicity of CIP in the nitrogen removal process of AS.

Fate of CIP in AS: implications for the impacts on receiving water bodies

Organic matter removal and biomass production in the three sets of bioreactors were determined by measuring sCOD and MLVSS, respectively, at steady state (days 28–70) (Fig. 5). The control showed $92 \pm 3\%$ and 0.8 ± 0.1 g/L for sCOD removal rate and MLVSS, respectively. The sCOD removal and MLVSS values were $88 \pm 3\%$ and 0.79 ± 0.17 g/L for the CIP_{50} communities and $88 \pm 2\%$ and 0.74 ± 0.1 g/L for the CIP_{500} communities, respectively, suggesting a slight decrease of both values in the CIP_{50} and CIP_{500} communities.

The CIP removal rates in the CIP-fed communities were followed for 70 days (Fig. 6a). Respective CIP removal of $74 \pm 2\%$ and $75 \pm 2\%$ was measured in the first feeding cycle of the CIP_{50} and CIP_{500}

communities, respectively. The values rapidly decreased to $22 \pm 3\%$ and $20 \pm 2\%$ at day 14 and then did not further change significantly over two months. Micropollutants in WWTPs can be removed via abiotic and biotic routes such as volatilization, photolysis, adsorption, and biotransformation. Here, the volatilization and photolysis of the CIP were likely negligible since CIP has a low Henry's constant $(5.09 \times 10^{-14}$ Pa·m^3/mol at 25 °C) (Sahlin et al. 2018) and long-term stability (i.e., non-detectable photolytic reactions) under normal sunlight (Wen et al. 2018). The activity of abiotic pathways was assessed in separate batch reactors (those without active biomass) under experimental conditions identical to those of the semi-continuous bioreactors. The batch tests showed non-detectable changes (< 1%) of CIP in the batch settings (data not shown), strongly suggesting negligible volatilization, hydrolysis, and photolysis. CIP in AS can be removed primarily via adsorption rather than biodegradation (Li and Zhang 2010). The persistence/resistance of CIP to biological breakdown is mainly attributable to its chemical properties. CIP contains fluoride and carboxyl functional groups, which render it resistant to biological catabolism (Tadkaew et al. 2011). Hence, we next determined the amount of CIP adsorbed on AS at steady state (at 42 days). The CIP concentrations were 16 ± 7 and 128 ± 45 μg/gVSS in the CIP_{50} and CIP_{500} communities (Fig. 6b), respectively, indicating a contribution of adsorption to the overall CIP removal. The total adsorbed amount (16–128 μg/gVSS) was higher than estimates by Zuccato et al. (2010), 2–510 μg/kg total suspended solids measured in sludge from full-scale WWTPs; this was likely due to the higher CIP loading (50–500 μg/L) in the influents used in this study than
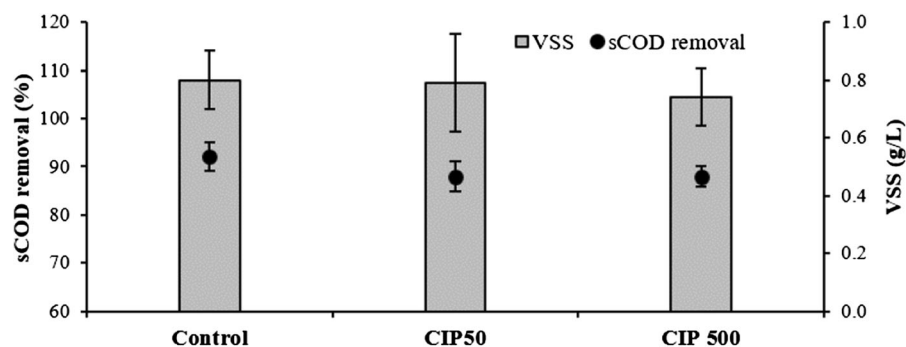
Fig. 5 COD removal ($n = 12$) and VSS ($n = 12$) concentrations at steady state (days 28–70). The bar/circle and error bar represent the mean and standard deviation, respectively

Fig. 6 CIP removal in representative feeding cycles over 70 days. **a** Time course of CIP removal in the CIP_{50} and CIP_{500} communities. Triplicate samples were measured for estimating the mean and standard deviation. **b** The total amount of CIP adsorbed onto AS at steady state. The bar and error bar represent the mean and standard deviation, respectively
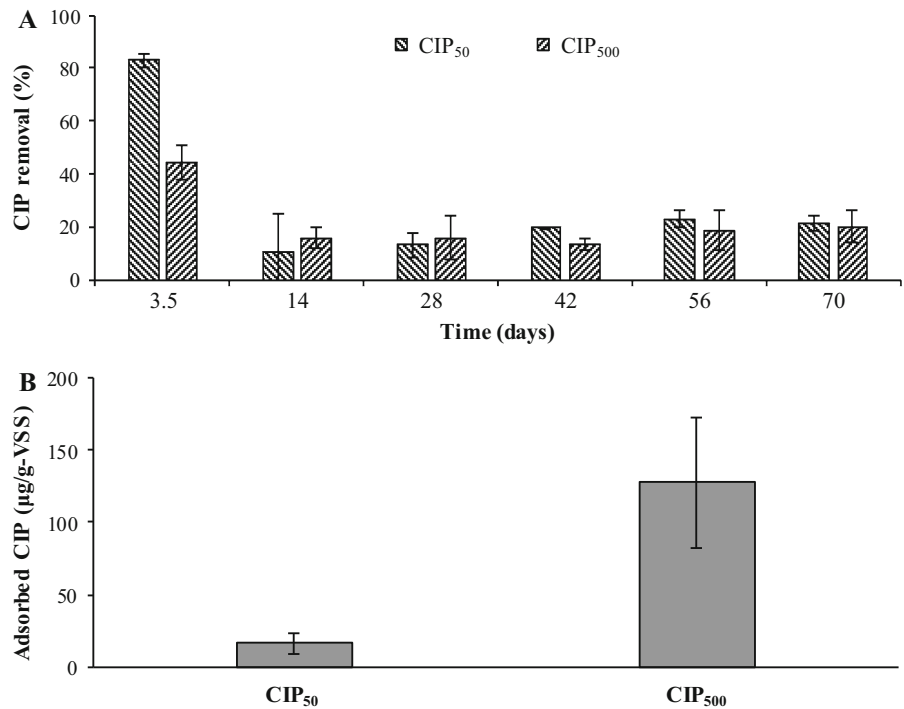
that in typical influents of WWTPs (e.g., < 10 μg/L). However, our adsorption values were comparable to those found by Mai et al. (2018), 2–462 μg/gVSS adsorbed to AS exposed to 0.05–50 mg/L of CIP.

While some WWTPs are capable of removing more than half of the CIP from effluents at lower input levels (e.g., up to 10 μg/L), our results suggest unsatisfactory CIP removal in CAS processes that receive influents with higher loads (50–500 μg/L) of CIP. However, this hypothesis needs to be tested with experimental verification in full-scale CAS processes where a number of factors (e.g., reactor configuration and sludge type) affect treatment efficiency. The degree of physicochemical sorption on biomass can be described with the adsorption–desorption distribution ratio (K_d, L/gVSS). We estimated the K_d values with the data shown in Fig. 6 using the equation: $K_d = X/(X_{VSS} \cdot S)$. X is the sorbed CIP concentration per unit volume of the reactor (mg/L), S is the CIP concentration (mg/L) assuming sorption equilibrium, and X_{VSS} is the VSS concentration (g/L) (Joss et al. 2006). The K_d values measured from the CIP_{50} and CIP_{500} reactors at steady state were 0.07 to 0.11 L/gVSS, respectively. Since < 2.5 log K_d is considered low sorption potential, our results (Fig. 6) were consistent with a study by

Nguyen et al. (2018) reporting nonsignificant sorption-mediated removal.

The biodegradation constant (K_{biol}, L/g-SS/day) can be used to represent the extent of biodegradability. Plósz et al. (2010) determined the K_{biol} value (0.55 L/g-SS/day) of CIP by aerobic AS, and a biodegradability classification scheme developed by Joss et al. (2006) suggests that a pollutant with $0.1 < K_{biol} < 10$ is partially biodegradable in conventional WWTPs. Based on those researchers' model simulations and the K_d and K_{biol} values estimated in our and other studies, wastewater bearing high levels of CIP (50–500 μg/L) can be expected to be partially treated (< 40%) by conventional complete mix- and plug-flow processes with typical operation conditions (e.g., 12 h of hydraulic retention time and 10–15 days of solid retention time). Therefore, the poor removal of CIP at 50–500 μg/L experimentally observed in our laboratory settings is consistent with the model prediction results based on the sorption and biodegradability parameters. Since a large body of literature reports potential ecological risks by CIP residuals, even at a few micrograms per liter level (Robinson et al. 2005; Johansson et al. 2014; Rico et al. 2014), the unsatisfactory CIP removal obtained in this study strongly suggests the need for alternative technologies to CAS

processes in WWTPs and more frequent monitoring campaigns on the occurrence and fate of CIP in receiving water bodies.

Conclusions

The results of this study revealed poor removal (20–22%) of CIP at 50–500 µg/L in AS, which implies that high levels of CIP carried with wastewater influents into CAS processes will not be treated to satisfactory levels that can ensure ecological safety in receiving water bodies. Further, 500 µg/L of CIP can cause significant shifts in the structure and diversity of AS microbial communities and is here shown to reduce core members (i.e., *Rhodobacteraceae* and *Nakamurellaceae*) in AS that play a key role in organic matter and nutrient removal; this is directly relevant to the system performance of biological WWTPs. We therefore strongly recommend further research on alternative treatment technologies and more frequent monitoring campaigns on the fate and occurrence of CIP in receiving water bodies.

References

APHA, AWWA, & WEF. (1998). *Standard methods for the examination of water and wastewater* (20th ed.). Washington DC: American Public Health Association/American Water Works Association/Water Environment Federation.

Bergaust, L., Mao, Y., Bakken, L., & Frostegård, A. (2010). Denitrification response patterns during the transition to anoxic respiration and posttranscriptional effects of suboptimal pH on nitrogen oxide reductase in Paracoccus denitrificans. *Applied and Environmental Microbiology*, 76, 6387–6396.

Cui, H., Wang, S. P., Fu, J., Zhou, Z. Q., Zhang, N., & Guo, L. (2014). Influence of ciprofloxacin on microbial community structure and function in soils. *Biology and Fertility of Soils, 50,* 939–947.

DeVries, S. L., & Zhang, P. (2016). Antibiotics and the terrestrial nitrogen cycle: A review. *Current Pollution Reports, 2*(1), 51–67.

Fick, J., Söderström, H., Lindberg, R. H., Phan, C., Tysklind, M., & Larsson, D. G. (2009). Contamination of surface, ground, and drinking water from pharmaceutical production. *Environmental Toxicology and Chemistry, 28*(12), 2522–2557.

Ghosh, W., George, A., Agarwal, A., Raj, P., Alam, M., Pyne, P., et al. (2011). Whole-genome shotgun sequencing of the sulfur-oxidizing chemoautotroph *Tetrathiobacter kashmirensis*. *Journal of Bacteriology, 193*(19), 5553–5554.

Girardi, C., Greve, J., Lamshöft, M., Fetzer, I., Miltner, A., Schäffer, A., et al. (2011). Biodegradation of ciprofloxacin in water and soil and its effects on the microbial communities. *Journal of Hazardous Materials, 198,* 22–30.

Goswami, M., Mangoli, S. H., & Jawali, N. (2006). Involvement of reactive oxygen species in the action of ciprofloxacin against *Escherichia coli*. *Antimicrobial Agents Chemotherapy, 50*(3), 949–954.

Isazadeh, S., Jauffur, S., & Frigon, D. (2016). Bacterial community assembly in activated sludge: Mapping beta diversity across environmental variables. *MicrobiologyOpen, 5,* 1050–10601.

Jiang, C., Geng, J., Hu, H., Ma, H., Gao, X., & Ren, H. (2017). Impact of selected non-steroidal anti-inflammatory pharmaceuticals on microbial community assembly and activity in sequencing batch reactors. *PLoS ONE, 12*(6), e0179236.

Johansson, C. H., Janmar, L., & Backhaus, T. (2014). Toxicity of ciprofloxacin and sulfamethoxazole to marine periphytic algae and bacteria. *Aquatic Toxicology, 156,* 248–258.

Joss, A., Zabczynski, S., Göbel, A., Hoffmann, B., Löffler, D., McArdell, C. S., et al. (2006). Biological degradation of pharmaceuticals in municipal wastewater treatment: proposing a classification scheme. *Water Research, 40*(8), 1686–1696.

Kozich, J. J., Westcott, S. L., Baxter, N. T., Highlander, S. K., & Schloss, P. D. (2013). Development of a dual-index sequencing strategy and curation pipeline for analyzing amplicon sequence data on the MiSeq Illumina sequencing platform. *Applied Environmental Microbiology, 79*(17), 5112–5120.

Larsson, D. G. J., de Pedro, C., & Paxeus, N. (2007). Effluent from drug manufactures contains extremely high levels of pharmaceuticals. *Journal of Hazardous Materials, 148*(3), 751–755.

Li, B., & Zhang, T. (2010). Biodegradation and adsorption of antibiotics in the activated sludge process. *Environmental Science and Technology, 44*(9), 3468–3473.

Mai, T. D., Stuckey, D. C., & Oh, S. (2018). Effect of ciprofloxacin on methane production and anaerobic microbial community. *Bioresource Technology, 261,* 240–248.

Nguyen, L. N., Nghiem, L. D., & Oh, S. (2018). Aerobic biotransformation of the antibiotic ciprofloxacin by Bradyrhizobium sp. isolated from activated sludge. *Chemosphere, 211,* 600–607.

Nguyen, L. N., & Oh, S. (2019). Impacts of antiseptic cetylpyridinium chloride on microbiome and its removal efficiency in aerobic activated sludge. *International Biodeterioration and Biodegradation, 137,* 23–29.

Nouioui, I., Göker, M., Carro, L., Montero-Calasanz, M. D., Rohde, M., Woyke, T., et al. (2017). High quality draft genome of *Nakamurella lactea* type strain, a rock actinobacterium, and emended description of *Nakamurella lactea*. *Standards in Genomic Sciences, 12,* 4. https://doi.org/10.1186/s40793-016-0216-0.

Oh, S., & Choi, D. (2018). Microbial community enhances biodegradation of bisphenol: A through selection of

Sphingomonadaceae. *Microbial Ecology*. https://doi.org/10.1007/s00248-018-1263-4.

Plósz, B. G., Leknes, H., & Thomas, K. V. (2010). Impacts of competitive inhibition, parent compound formation and partitioning behavior on the removal of antibiotics in municipal wastewater treatment. *Environmental Science and Technology, 44*(2), 734–742.

Rico, A., Dimitrov, M. R., Van Wijngaarden, R. P., Satapornvanit, K., Smidt, H., & Van den Brink, P. J. (2014). Effects of the antibiotic enrofloxacin on the ecology of tropical eutrophic freshwater microcosms. *Aquatic Toxicology, 147,* 92–104.

Robinson, A. A., Belden, J. B., & Lydy, M. J. (2005). Toxicity of fluoroquinolone antibiotics to aquatic organisms. *Environmental Toxicology and Chemistry, 24*(2), 423–430.

Sahlin, S., Joakim Larsson, D. G., & Ågerstrand, M. (2018). Ciprofloxacin: EQS data overview. The Department of Environmental Science and Analytical Chemistry (ACES) Report 15. Stockholm: Stockholm University

Saunders, A. M., Albertsen, M., Vollertsen, J., & Nielsen, P. H. (2016). The activated sludge ecosystem contains a core community of abundant organisms. *ISME Journal, 10,* 11–20.

Shchegolkova, N. M., Krasnov, G. S., Belova, A. A., Dmitriev, A. A., Kharitonov, S. L., Klimina, K. M., et al. (2016). Microbial community structure of activated sludge in treatment plants with different wastewater compositions. *Frontiers in Microbiology, 7,* 90. https://doi.org/10.3389/fmicb.2016.00090.

Stokholm-Bjerregaard, M., McIlroy, S. J., Nierychlo, M., Karst, S. M., Albertsen, M., & Nielsen, P. H. (2017). A critical assessment of the microorganisms proposed to be important to enhanced biological phosphorus removal in full-scale wastewater treatment systems. *Frontiers in Microbiology, 8,* 718. https://doi.org/10.3389/fmicb.2017.00718.

Tadkaew, N., Hai, F. I., McDonald, J. A., Khan, S. J., & Nghiem, L. D. (2011). Removal of trace organics by MBR treatment: The role of molecular properties. *Water Research, 45*(8), 2439–2451.

Verlicchi, P., Al Aukidy, M., & Zambello, E. (2012). Occurrence of pharmaceutical compounds in urban wastewater: Removal, mass load and environmental risk after a secondary treatment–a review. *Science of the Total Environment, 429,* 123–155.

Wen, X.-J., Niu, C.-G., Zhang, L., Liang, C., Guo, H., & Zeng, G.-M. (2018). Photocatalytic degradation of ciprofloxacin by a novel Z-scheme CeO$_2$-Ag/AgBr photocatalyst: Influencing factors, possible degradation pathways, and mechanism insight. *Journal of Catalysis, 358,* 141–154.

Werner, J. J., Knights, D., Garcia, M. L., Scalfone, N. B., Smith, S., Yarasheski, K., et al. (2011). Bacterial community structures are unique and resilient in full-scale bioenergy systems. *Proceedings of the National Academy of Sciences of the United States of America, 108*(10), 4158–4163.

Wijekoon, K. C., Hai, F. I., Kang, J., Price, W. E., Guo, W., Ngo, H. H., et al. (2013). The fate of pharmaceuticals, steroid hormones, phytoestrogens, UV-filters and pesticides during MBR treatment. *Bioresource Technology, 144,* 247–254.

Yi, K., Wang, D., Qi, Y., Li, X., Chen, H., Sun, J., et al. (2017). Effect of ciprofloxacin on biological nitrogen and phosphorus removal from wastewater. *Science of the Total Environment, 605–606,* 368–375.

Yoshimi, Y., Hiraishi, A., & Nakamura, L. (1996). Isolation and characterization of *Microsphaera multipartita* gen. nov., sp. nov., a polysaccharide-accumulating Gram-positive bacterium from activated sludge. *International Journal of Systematic Bacteriology, 46,* 519–525.

Zhang, B., Xu, X., & Zhu, L. (2018). Activated sludge bacterial communities of typical wastewater treatment plants: Distinct genera identification and metabolic potential differential analysis. *AMB Express, 8*(1), 184.

Zhou, J., & Ning, D. (2017). Stochastic community assembly: Does it matter in microbial ecology? *Microbiology and Molecular Biology Reviews, 81,* e00002–e00017. https://doi.org/10.1128/MMBR.00002-17.

Zielińska, M., Rusanowska, P., Jarząbek, J., & Nielsen, J. L. (2016). Community dynamics of denitrifying bacteria in full-scale wastewater treatment plants. *Environmental Technology, 37*(18), 2358–2367.

Zuccato, E., Castiglioni, S., Bagnati, R., Melis, M., & Fanelli, R. (2010). Source, occurrence and fate of antibiotics in the Italian aquatic environment. *Journal of Hazardous Materials, 179*(1–3), 1042–1048.